Velocity estimation and comparison of two insect vision based motion detection models

Sreeja Rajesh[a], David O'Carroll[a] and Derek Abbott[b]

[a]Department of Physiology and Department of Electrical & Electronic Engineering and
Centre for Biomedical Engineering, Adelaide University, SA-5005, Australia
[b]Department of Electrical & Electronic Engineering and
Centre for Biomedical Engineering, Adelaide University, SA-5005, Australia

ABSTRACT

Insects are blessed with a very efficient yet simple visual system which enable them to navigate with great ease and accuracy. Though a lot has been done in the field of insect vision, there is still not a clear understanding of how velocity is determined in biological vision systems. The dominant model for insect motion detection, first proposed by Hassentein and Reichardt in 1956 has gained widespread acceptance in the invertebrate vision community. The template model, proposed later by Horridge in 1990, permits simple tracking techniques and lends itself easily to both hardware and software. Analysis and simulations by Dror suggest that the inclusion of additional system components to perform pre-filtering, response compression, integration and adaptation, to a basic Reichardt correlator can make it less sensitive to contrast and spatial structure thereby providing a more robust estimate of local image velocity. It was found from the data obtained, from the intracellular recordings of the steady state responses of wide field neurons in the hoverfly *Volucella*, that the shape of the curves obtained, agreed perfectly with the theoretical predictions made by Dror. In order to compare it with the template model, an experiment was done to get the velocity response curves of the template model using the same image statistics. The results leads us to believe that the fly motion detector emulates a modified Reichardt correlator.

Keywords: Reichardt correlator, template model, motion detection, velocity estimation

1. INTRODUCTION

Anyone who has watched a group of bees flying together, would be marveled by their amazing ability to fly with such great speed without colliding into one another. The activities of insects clearly reveal the extraordinary navigational skills that the insects possess despite the fact that they have a very simple visual system. The study of the insect visual system has offered solutions to a number of problems faced by the conventional machine vision systems and has led to many elegant strategies that can be profitably applied to motion detection,[1] velocity estimation,[2] and has even be used in the design of collision avoidance sensors[3] and autonomous

Further author information: (Send correspondence to Sreeja Rajesh)
Sreeja Rajesh: E-mail: srajesh@eleceng.adelaide.edu.au, Telephone: 83036296
David O'Carroll: E-mail: david.ocarroll@adelaide.edu.au
Derek Abbott: E-mail: dabbott@eleceng.adelaide.edu.au

Smart Materials, Structures, and Systems, S. Mohan, B. Dattaguru,
S. Gopalakrishnan, Editors, Proceedings of SPIE Vol. 5062 (2003)

robots.[4] Research over several decades has revealed that the visual system of insects are exquisitely sensitive to motion. The study of the visual system of insects has inspired many models of motion detection.

The earliest and probably the most famous model of motion detection inspired by biological systems was developed by Reichardt and Hassentein[5] in 1956 after a series of behavioural experiments examining the opto-motor response of insects. The Reichardt or correlation motion detector possess a highly parallel architecture. Each elementary motion detector (EMD) detects motion in a preferred direction by comparing a signal from one receptor with a delayed signal from an adjacent receptor. The comparison is performed using a nonlinear, multiplicative, interaction between the two channels. Two EMDs tuned to opposite direction are combined to form a bidirectional motion detector. The multiplicative interaction employed in this detector is an excitory mechanism. In 1965, Barlow and Levick[6] pointed out that an inhibitory mechanism was also capable of providing directionally selective motion detection. In 1974, a linear lateral inhibition model was proposed by Hartline and Ratliff[7] as a result of the experiments on the compound eye of *limulus*. However, in order to be able to model directional selectivity for motion detection, nonlinear interactions are required. In 1984, Pinter[8,9] came up with the multiplicative lateral inhibition model, which is also known as the shunting inhibition model that was introduced to provide directional selectivity and also to describe observations regarding the variation of the shape and size of the receptive fields with changing light intensity.

Many structurally different biological motion detection models were proposed by either adding temporal, spatial or spatio-temporal filters before applying the input to the EMD cell or by adding spatial or temporal feedback to enhance the adaptability to mean luminance, again before the EMD units.

In 1990, after conducting many experimental studies on the behaviour of the insect visual system, Horridge[10,11] proposed a simplified model of the insect visual system called the template model. This empirical model compares the contrast between two adjacent receptors, at two sampling instances, to form a 2×2 template. These templates can give simple directional information. Operations are performed mainly between adjacent receptors, which make this model easy to implement in a parallel architecture. Several generations of insect vision chips based on the template model have been developed by Moini *et al.*[12–14]

Most of these spatio temporal models, currently the dominant models for motion detection in vertebrates, are mathematically equivalent to correlator models.[15] Correlator models have been applied to explain motion detection in humans, birds and cats.[16–18] In the absence of additional system components or assumptions, the raw output of a basic Reichardt correlator provides an inaccurate, ambiguous indication of image velocity.[19] But it has been found that the use of various forms of spatial filtering, temporal filtering, saturation, integration and adaptation within the motion detection system may improve the performance of the correlator based system in response to many stimuli, including complex natural images. In this paper, we have used experimental results on the fly as a model organism to confirm these predictions. The fly is chosen as a model organism here for both experiments as well as computational simulations due to the abundance of behavioural, anatomical and electrophysiological data available for its motion detection. We have also conducted an experiment to compare the response of the template model with the elaborated Reichardt correlator using the same image statistics. Since the template model produces templates as its response, the velocity versus the number of templates curve that we get, agrees with the experimental results on the fly. As the template model is structurally similar to an EMD, we can say that the basic fly motion detector follows a modified Reichardt correlator.

2. REICHARDT CORRELATOR MODEL

Fig. 1 shows a simplified version of the correlator model which is the earliest and the best known model proposed by Hassenstein and Reichardt in 1956.[5] Both behavioural and physiological experiments on insect visual system indicate that movement detection occurs between neighbouring points of the sampling lattice of the eye. This implies that a motion detector has two input channels and the two channels should possess an asymmetric arrangement. Asymmetry is necessary for the detector to acquire direction selectivity. Furthermore the interaction between two channels must be nonlinear if the detector is to respond selectively to moving gratings. The asymmetrically nonlinear interaction between two input channels is termed the elementary motion detector (EMD).[20] Such an EMD will elicit a strong response when a visual stimulus moves in a specified

direction (the preferred direction) and a weak response when the stimulus moves in the opposite direction as shown in Fig. 1.

A basic Reichardt correlator is formed by combining two EMDs that are tuned to opposite direction, to indicate bidirectional motion. The nonlinear interaction is assumed to be a multiplication, M, which is the simplest possible nonlinear interaction. The asymmetry is implemented by using a delayed unit, τ, which is the time constant of a first order low pass filter. This filter acts as a delayed element. The input channels are spatially separated by an angular distance, $\Delta\phi$. The outputs of the two multiplications are subtracted to give a single time-dependent correlator output.

Though insects and humans appear to be capable of estimating image velocities,[21,22] the basic correlator model does not function as a velocity estimator. It reliably indicates directional motion of sinusoidal gratings, but the response depends on contrast (brightness) and spatial frequency (shape) as well as velocity.[19]

But by modifying the basic correlator to include spatial and temporal pre-filtering, compression, integration and adaptation, the correlator based system can be made to function as a velocity estimator.[23]

3. THE TEMPLATE MODEL

The template model proposed by Horridge[10,11] models the function of the small field motion detection neurons in the *medulla*. In the template model the temporal contrast of the adjacent cells at consecutive instances are used to determine the direction of motion of an object. For simplicity, only temporal contrast at two instants and from two neighbouring cells is considered.

The visual field is sampled spatially. Each sampling channel detects changes in light intensity at two consecutive sampling instances to show either an increase ($\uparrow$), a decrease ($\downarrow$) or a no change ($-$). Adjacent photoreceptors carry out the detection of directional motion in insects and thus by copying this mechanism, the changed states are spatially combined between adjacent channels. Hence for a pair of adjacent sampling channels, there are 9 possible combinations:

$(- -)$, $(\uparrow -)$, $(\uparrow \uparrow)$, $(\uparrow \downarrow)$, $(\downarrow -)$, $(\downarrow \downarrow)$, $(- \downarrow)$, $(\downarrow \uparrow)$, $(- \uparrow)$.

Since in any visual system directional motion is accomplished as a spatio-temporal operation, the temporal domain is included by associating the combinations obtained at two consecutive sampling times t_0 and t_1, thus yielding 81 spatio-temporal combinations or templates. Thus the temporal contrast of two neighbouring cells, at two sampling instances, are combined to give simple motion measures called "templates".

Out of these 81 templates, there are only 8 templates, which indicate coherent motion. The templates sensitive to coherent motion are the ones in which one of the four entries is no change in intensity and the other three must identically either increase or decrease in intensity. These templates are known as directionally motion sensitive templates (DMSTs).[24] These templates possess the 3:1 diagonally symmetric structure. The DMSTs are named using the first eight alphabetic characters, from 'A' to 'H'. The templates having one intensity change entries and three no change entries are purely generated by motion – they occur at the concave corners of the staircase motion trajectory.[25] In other words, they occur simultaneously in pairs with the DMSTs at each sampling instance. They indicate the current position of the moving object and hence are referred to as the position conjugate templates (PCTs). The PCTs indicate the location of their DMST counterparts, which occur at the next sampling instant. The pair of DMSTs and corresponding PCTs are referred to as 'conjugate pairs of templates'. The PCTs are named using the numeric character from '1' to '8'.

The template model is easily implemented in VLSI, because the thresholding and template formation operations are simple and can be done in parallel. The presence of only three states reduces the bandwidth requirements compared to other vision systems. A series of bugeye chips[12–14] were implemented based on the template model.

In the software implementation of the template model, the array of on-chip photodetectors is replaced by a CMOS camera. The filtering operation in the lamina layer was implemented using temporal differentiation in the custom chips; whilst in our CMOS camera prototype this is performed using simple frame differencing. The CMOS camera is interfaced to a personal computer and the captured image is stored in the buffers. The

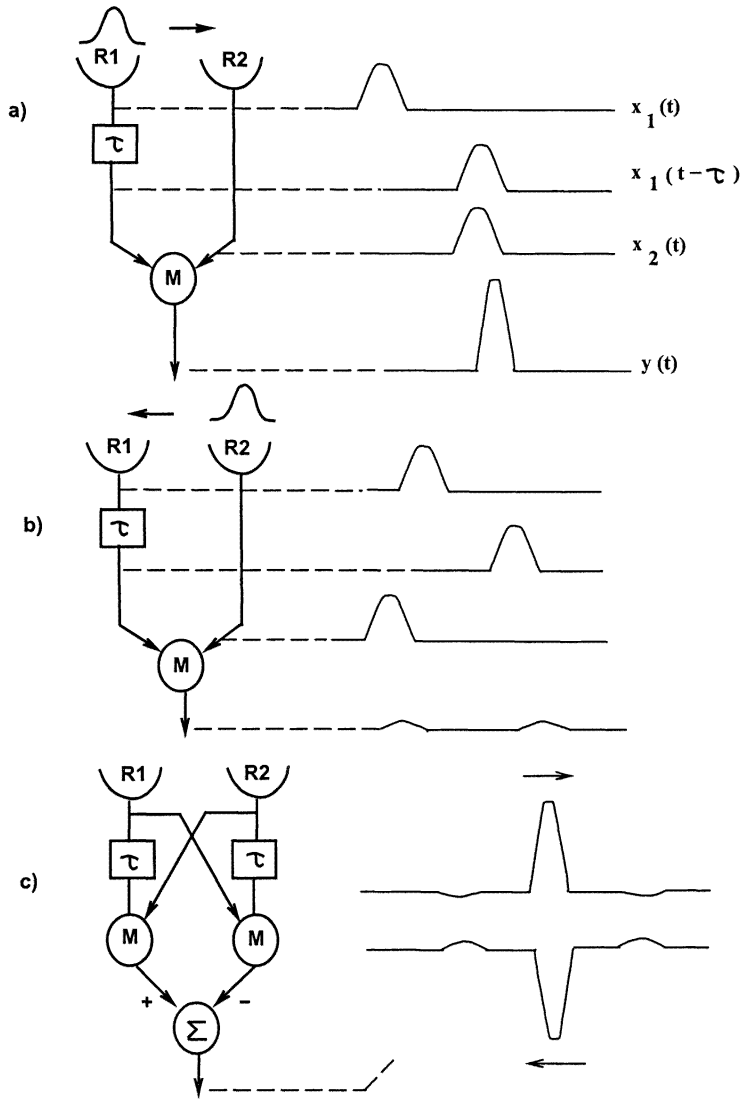

Fig. 1. Schematic representation of the correlation model. $\Delta\phi$ is the sampling base of the detector. R1 and R2 denote two adjacent photoreceptors, the τ-box represents a temporal delay unit, and the M-unit is the multiplication stage. a) Response of the EMD (subunit) to a movement in a preferred direction. b) Response in the null direction. c) Responses of the basic correlator to movement in either directions.

difference between the current image in the current frame buffer and the previous image in the previous frame buffer will give changes in the motion, which are thresholded and stored as templates. Template generation here is performed in software whereas some custom chips have template generation elements in the hardware. Thus by comparing the templates obtained from frame differencing with directionally sensitive motion templates, the direction of motion of the moving object can be obtained. These templates can be used to measure the velocity of moving objects. Experimental results show that a moving object or edge causes the same template to occur consistently at subsequent time steps. The angular velocity may be estimated by evaluating the ratio of the

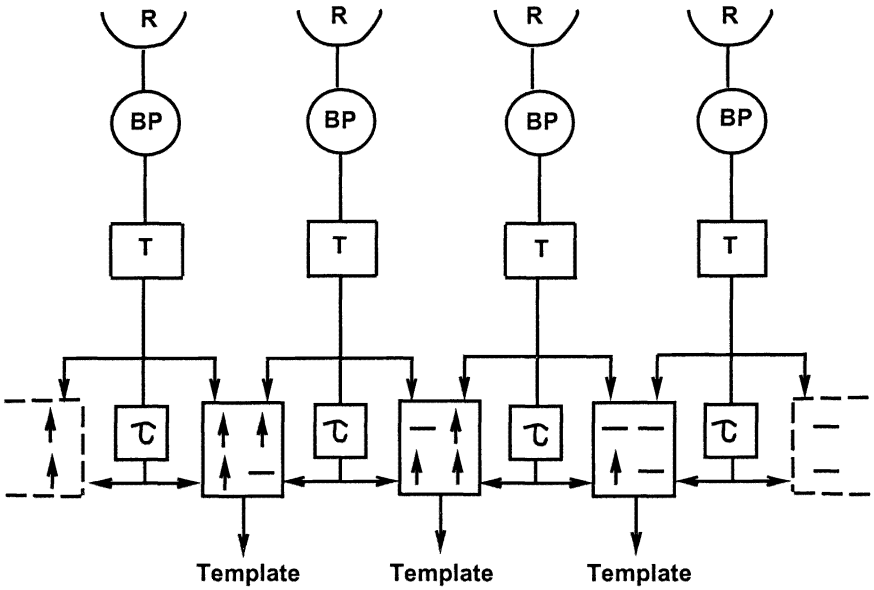

Fig. 2. Schematic representation of the template model. The R units represent the photoreceptors, the BP-units denote the band pass filters to detect changes in intensity, the T-boxes represent the thresholding units. The τ-boxes denote the temporal delay units with an amount of time τ.

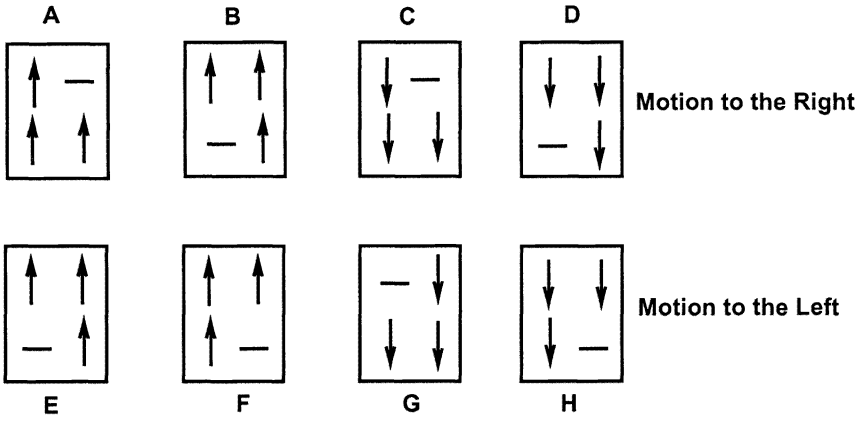

Fig. 3: Directionally Motion Sensitive Templates

displacement of a motion sensitive template, to the time between the template's occurrences.[26]

4. VELOCITY ESTIMATION

Velocity information of moving objects is widely used in a number of applications. This information can contribute to scene interpretation such as recovering the structure of the environment, estimating time to contact or range for obstacle avoidance, segmenting images and predicting future location of moving objects. A basic Reichardt correlator does not act as a good velocity estimator because its response depends on contrast and spatial frequency as well as velocity. Analysis and simulations suggest that the processes commonly found in visual systems, such as pre-filtering, response compression, integration, and adaptation, improve the reliability of velocity estimation by Reichardt correlator and expand the range of velocities coded. To prove this experimentally, a set of experiments were carried out in which the recordings of steady-state responses of wide-field neurons in a hoverfly to motion of broad-band images at different velocities was taken and compared with the

analytical and computational predictions. Additional processing may occur subsequent to or in parallel with the wide-field neurons, so we are not necessarily measuring the fly's actual perception of velocity. However, because the wide-field neurons perform extensive spatial integration and because recorded output is averaged over time, the results are effectively velocity response curves for wide-field neurons.

Male specimens of the hoverfly *Volucella* are used for these experiments. The wide field neurons have proven particularly amenable to physiological analysis because their structure and physiological characteristics are nearly identical in different animals.[27] Intracellular recordings from wide field cells indicate that they sum the outputs of local Reichardt correlators in their receptive fields. The HS cells or the Horizontal System typically consists of three horizontal cells termed north (HSN), equatorial (HSE), and south (HSS) horizontal cells because their dendritic trees cover the dorsal, medial and ventral regions of the lobula plate, respectively, with corresponding physiological receptive fields.

Here we have taken recordings from HSN, HSNE, and HSE neurons which are tangential cells of the horizontal system. (In syrphids such as *volucella*, the HS system consists of four neurons - an HSNE neuron in addition to the three HS neurons mentioned). All three of these neurons have dorsal receptive fields. They exhibit graded responses, with horizontal progressive motion eliciting maximum depolarization. Instead of natural images, random texture fields generated by a Picasso Image Synthesizer and a Dual Channel Velocity Field and Stereogram Generator under control of a Macintosh computer are used. Modifications to both the Image Synthesizer and the Stereogram Generator allowed the display of moving texture fields at a video frame rate of 300 Hz with a variable raster rate on a Tektronix 608 XYZ display. The random textures consist of horizontal rectangular texture elements ("texels") each of which has an equal probability of being illuminated at the display's maximum intensity or not being illuminated at all. By varying a texture density parameter, texels of 4 different sizes (widths 10.3, 5.2, 2.6, and 1.3 mm/texel) can be used. In addition, by lowering the frame rate to 200 Hz and increasing the raster rate, we can decrease the texel size to 0.86 or 0.67 mm/texel. The apparent size of a texel and the perceived angular velocity depend on the distance of the moving pattern from the fly. The display is generally positioned at about 6 cm from the fly's eyes and the precise distance was recorded for each experiment in order to calculate angular velocity and angular texture density. Texels thus subtended angles ranging from 0.64° (less than the inter-ommatidial angle of the fly) to 9.7° (nearly ten times that angle).

The mean horizontal power spectral density for a row of a random texture image with texel width θ°/texel is given by[23]:

$$P(f_s) = \theta \frac{\sin^2(\pi f_s \theta)}{(\pi f_s \theta)^2}. \quad (1)$$

4.1. Model Correlator Response

Fig. 4 shows velocity response curves for a model correlator predicted analytically from the power spectra of random textures of different densities. This correlator model included spatial blurring by the optics and temporal filtering by light-adapted photoreceptors and LMCs. Saturation effects were not included because the texels themselves provide a binary-valued input signal. The exact shape of the curves and their peak response velocities depend on a number of parameters which are difficult to predict on the basis of available data for these cells, such as the extent of temporal high-pass filtering. Moreover, the predicted curves in this figure do not take account of known nonlinear effects such as gain control. However several important features of the curves can be predicted with confidence. First, they will have the same general shape as the curves predicted for natural images, increasing monotonically up to a peak response velocity and then falling off. Second, the velocity response curves should shift to the left as texture density increases. Since the luminous intensities of the display could not be adjusted for either illuminated or unilluminated texels, most of the stimuli had a very high contrast of 94%, and a mean luminance of 37 Cd/m^2. In some later experiments, luminance was increased and the stimulus contrast was decreased by adding uniform foreground illumination from one or more light sources. The responses of HS cells to progressive horizontal image motion at 25 approximately logarithmically spaced velocities between 7 and 1800°/s was recorded, with the precise velocity range depending on frame rate and screen distance. 200 ms presentations of image motion at each velocity were interleaved with 200 ms adapting stimuli at an angular velocity 400°/s. The last 100 ms of the response at each velocity was averaged to obtain a single response value. To control for effects of adaptation during the experiment, the test stimuli

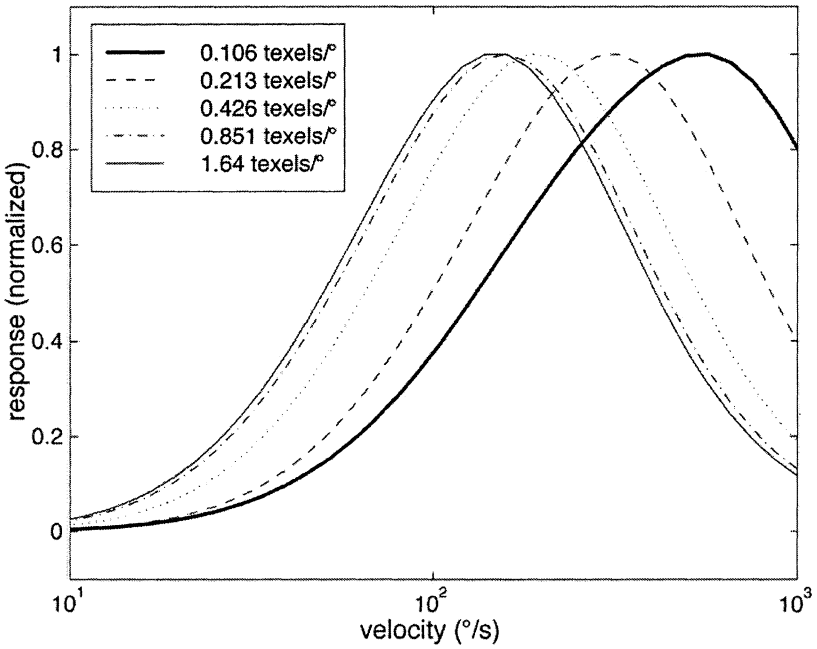

Fig. 4. Velocity response curves measured at six different texture densities for a single HSNE neuron. As density increases, the mean horizontal power spectrum of the texture field becomes flatter and the velocity response curves shift to the left. The legend indicates texture density and the number of measurements averaged to obtain each point in the figure. The magnitude of responses of the cell at different texture densities differed significantly, but the curves presented here have been normalised for comparison.

were presented in a monotonically increasing sequence of velocities, followed by a monotonically decreasing sequence. This protocol was designed to obtain quick measurements while maintaining the cell in a state of uniform adaptation. The protocol was repeated three or more times for a given texture and obtained a single velocity response curve by averaging the responses to motion at each velocity.

4.2. Response of the wide field neurons of the hoverfly

Fig. 5 shows velocity response curves for one HSNE neuron measured at six texture densities. The velocity response curves show the expected shape, rising to a peak response at some optimum velocity and then falling off again. The tuning curves for broad-band images have higher optimal velocities than the corresponding tuning curves for sinusoidal gratings of optimal spatial frequency. As texture density increases, the curves shift to the left, with the optimal velocity decreasing from over 300°/s to 100°/s over the range of densities used. As predicted by the model of Fig. 4, the curves cease to shift left at the very highest densities, as the image power spectrum becomes almost completely flat in the relevant frequency range. The model predicts qualitative aspects of the recorded data surprisingly well, given that model parameters were literature values for typical large hoverflies and were not tuned to the cell in question. The data of Fig. 5 represents a particularly successful recording session lasting over 2 hours, during which response curves at a wide range of densities were measured and test protocols were repeated twice at most densities. Neurons in other animals gave similar results, but typically with more noise due to shorter recording sessions.

Fig. 6 indicates the relationship between texture density and optimum velocity for a number of HS cells from several flies, as well as analytical predictions. With one notable anomaly, all cells show the expected decrease of optimum velocity with increasing density. The velocity optima do differ systematically from cell to cell. At any given texture density, some neurons have optimal velocities 50% greater than those of others. These systematic variations between cells may reflect real variations in physiology; for example, temporal prefiltering might vary between organisms or regions of the visual field, which could explain the differences shown. Alternatively, the

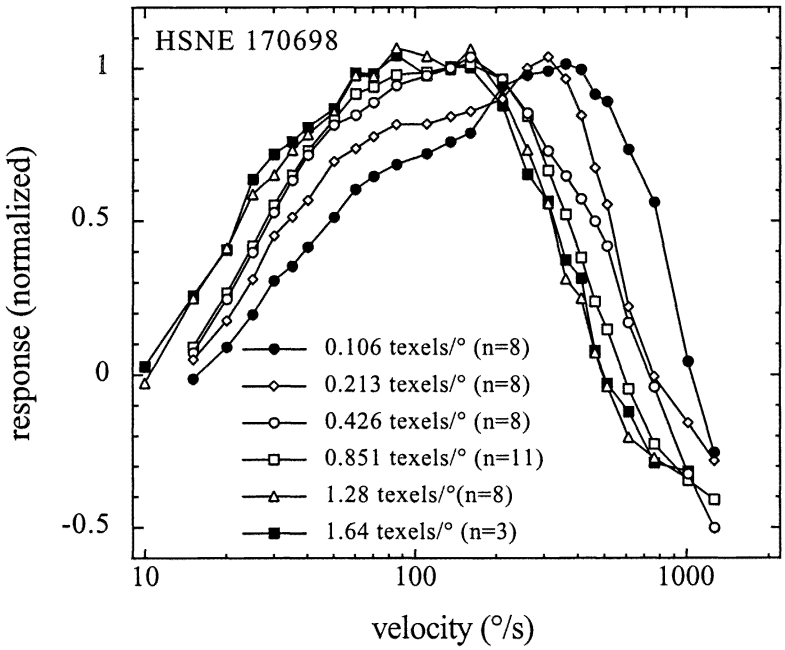

Fig. 5. Velocity response curves measured at six different texture densities for a single HSNE neuron. As density increases, the mean horizontal power spectrum of the texture field becomes flatter and the velocity response curves shift to the left. The legend indicates texture density and the number of measurements averaged to obtain each point in the figure. The magnitude of responses of the cell at different texture densities differed significantly, but the curves presented here have been normalised for comparison.

variations may be due to differences in the recordings, such as the position of the screen relative to the receptive field. Velocity tuning curves as well as spatial and temporal frequency tuning curves were compared for HSE, HSNE, and HSN neurons, but no significant systematic differences were found.

4.3. Template model response

We have set up an experiment to compare the velocity response curve of the Reichardt correlator with that of the template model. In this experiment, the camera was placed in the centre of a hollow cylinder with random horizontal texture elements ("texels") printed on a horizontal roll of paper stuck inside. The cylinder is motor controlled and the angular speed of the cylinder can be adjusted by changing the voltage supply to the motor. Our program then tried to count the number of templates produced, by detecting the motion of the texels. By varying the texure density parameter, texels of 4 different sizes can be used. The experiment is repeated for each texture density. Since the template model gives us templates as its response, the velocity response curve in this case is the velocity versus number of templates, which is plotted for each texel density. Although the Horridge model is essentially a discrete-time model, the front end of the true Horridge model does a continuous-time differentiation and then the signal is digitised. However, in the set-up with the texels and video camera, that implementation of the Horridge model is full discrete-time. That could be the reason why the results do not show an exact similarity with the Reichardt model and the experiments done on the fly. But since basically the template model is developed from an EMD, which is the minimum prerequisite for directionally selective motion detection in a visual system, we see that the curves do agree to some extent with the Reichardt correlator.

Fig. 7 shows the velocity response curves measured at five texture densities using the template model algorithm. The template model detects the motion of objects as edges. When the texel density is low, the texels are bigger and fewer in number, hence there are a fewer number of edges and thereby a fewer number of templates at low velocities. But as the texel density increases, the number of edges detected and the number of templates increases resulting in the curve shifting to the left, showing similarity in response to the response

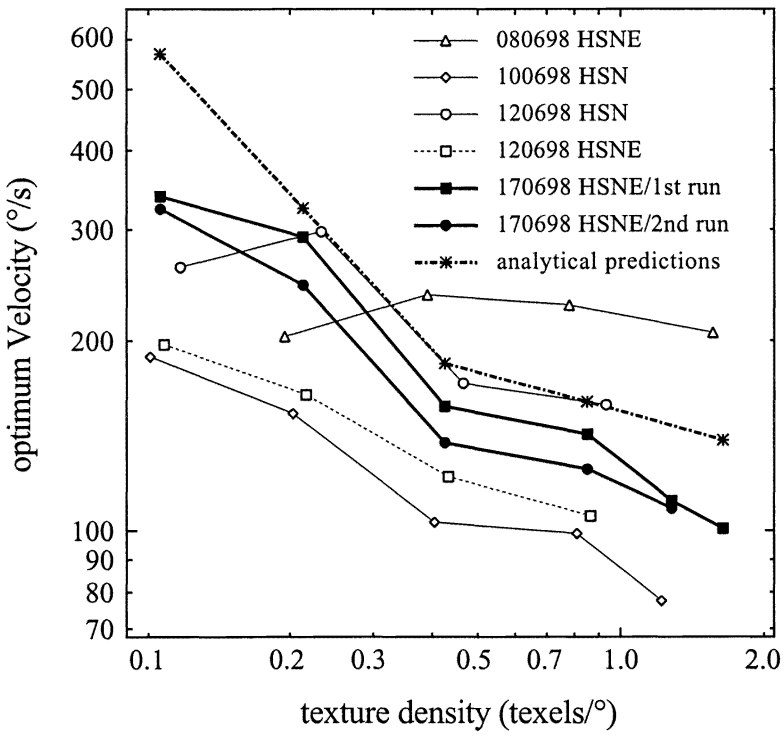

Fig. 6. Optimum velocity as a function of texture density for several neurons. The optimal velocity is the velocity of pattern motion for which the neuron gives a maximum steady-state response; this velocity generally decreases as texture density increases, in agreement with theoretical predictions. Neuron 080698 HSNE exhibited anomalous behaviour, while a noisy velocity response curve led to a single anomalous measurement for neuron 120698 HSN at the second lowest texture density. The legends indicate the type of each neuron. In order to reduce the effects of measurement noise, we estimated the velocity optimum for each cell at each texture density as the velocity optimum of a second-order thin-plate spline fit to the velocity response curve on a logarithmic velocity axis. The amplitude of the curve corresponding to analytical predictions is highly sensitive to the properties of the high-pass temporal prefilter. A slightly weaker high-pass temporal prefilter or the addition of a realistic high-pass spatial prefilter would decrease the predicted response velocities into the range of those observed experimentally.

of the HSNE neuron. As the texel density increases, it is seen that the response increases then begins to fall. This is due to the blurring effect caused by the fast motion of the texels. The higher the texel density, the blur occurs at progressively lower velocities. But as we increase the velocity, more texels pass in front of the camera at a faster rate, resulting in increase of the response again and then further increase in velocity causes more motion blur resulting in decrease of response. The similarities that we can see, when we compare the response to that of the HSNE nueron of the fly and the Reichardt model is that the curves shift to the left as the texel density increases. The response also becomes flatter as the texel density increases similar to the response of the wide field neuron of the fly.

In the template model, experimental results show that a moving object (or edge) consistently causes the same motion sensitive template to occur at subsequent time steps, and at positions corresponding to the displacement of the edge relative to the detector.[26] The angular velocity may be estimated by evaluating the ratio of the displacement of a motion sensitive template, to the time between the template's occurrences. In Fig 8, the horizontal axes represents the angular velocity measured using a tachometer and the verticle axis represents the velocity measured, by tracking of the templates, done by the template model algorithm. At lower velocities it is seen that the algorithm gives a correct measure of the velocity as the response coincides with the ideal response, but as the velocity increases the blurring of the texels causes the response to deviate from the ideal line.

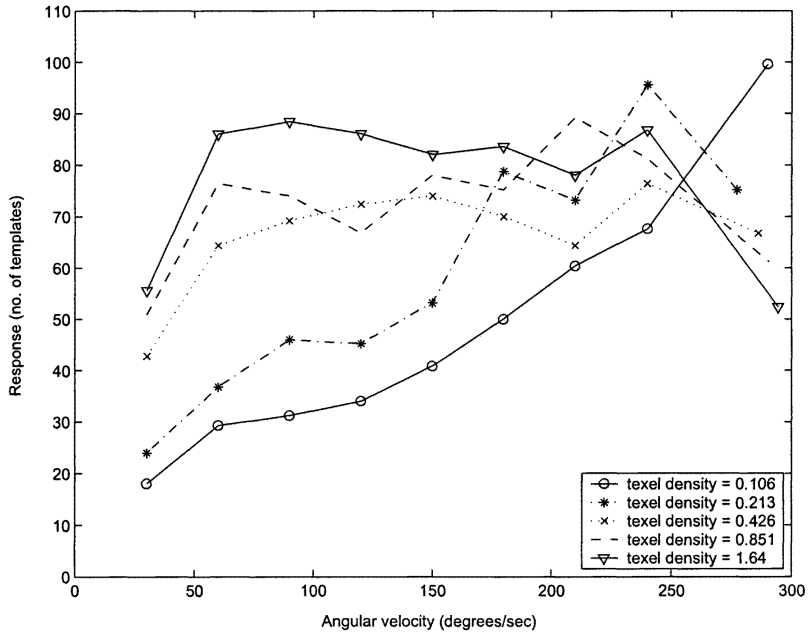

Fig. 7. Velocity response curves measured at six different texture densities for the template model. As density increases, the number of templates produced increases causing the velocity response curve to shift to the left, emulating the Reichardt model response. The shape of the curve obtained differs to the response obtained from a Reichardt correlator or HSNE neuron of the fly. A number of reasons could be attributed to this. The implementation of the Horridge model here is a discrete time model, whereas the Reichardt correlator is an analog model. It could also be due to the noise introduced from the camera and during the analog to digital conversion, and it could also be due to the motion blur caused by the camera.

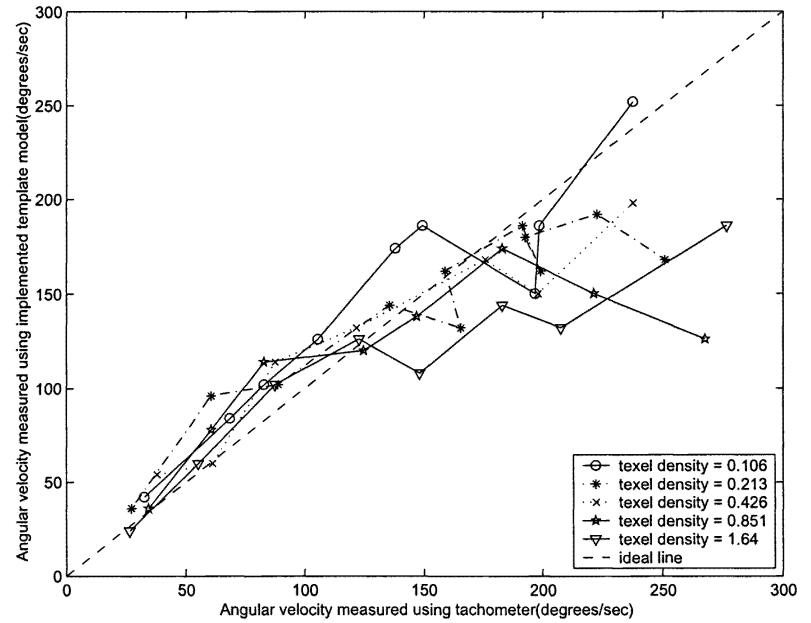

Fig. 8. Benchmark angular velocity measured by the tachometer versus benchmark velocity measured using the implemented template model. The angular velocity measured by the algorithm deviates from the actual measured velocity or the ideal line for all texel densities at higher velocities. As the texel density increases it is found that the velocity from which the deviation from the ideal line starts to occur, decreases.

5. CONCLUSION

This study analyses the important aspects of accurately estimating the local image velocity using a Reichardt correlator and template model. It is found that both these models give correct estimate of velocity at low velocities and their efficiency decreases at higher velocities. It also proves that experimentally supported elaborations of the basic Reichardt correlator enhances its reliability as a velocity estimator. Since the basic principle of a template model is the same as the Reichardt correlator, the elaborated Reichardt correlator and the template model produce similar response. This result has been verified by the data obtained from the experiments done on the wide field neurons of the hoverfly which qualitatively matches the above two results in several important aspects. But you can find that there is more similarity with the elaborated Reichardt correlator response than with the template model result.

It has also been found that many physiological mechanisms, such as contrast normalisation and adaptation could further improve the performance of the velocity estimation system. Future work in this area could be to include many other experimentally observed phenomena like output gain control, signal rectification and various other forms of adaptation in model simulation and to study their effects on the accuracy of velocity estimation. Since visual scenes do not generally translate rigidly at fixed velocity with respect to the retina, the next challenge could be to incorporate three dimensional space time power spectra of natural image sequences into computer algorithms for local velocity estimation.

ACKNOWLEDGMENTS

Funding from the US Air force Research Laboratory / Asian Office for Aerospace Research & Development (contract # F62562-01-P-0158), the Sir Ross & Sir Keith Smith Fund and the Australian Research Council is gratefully acknowledged.

REFERENCES

1. R. R. Harrison and C. Koch, "A robust analog VLSI Reichardt motion sensor," *Analog Integrated Circuits and Signal Processing* **24**(3), pp. 213–229, 2000.
2. X. T. Nguyen, A. Bouzerdoum, and A. Moini, "Velocity measurement using a smart micro-sensor," *International Symposium on Robotics and Cybernetics,* Lille, France **943**, pp. 937–942, 1996.
3. D. C. Goodfellow and D. Abbott, "Millimeter-wave insect vision sensors for collision avoidance in space," *Proceedings of the SPIE conference on The International Society for Optical Engineering* **3838**, pp. 217–225, 1999.
4. M. V. Srinivasan, J. S. Chahl, K. Weber, a. M. G. N. S. Venkatesh, and S. W. Zhang, "Robot navigation inspired by principles of insect vision," *Robotics and Autonomous Systems* **26**, pp. 203–216, 1998.
5. B. Hassenstein and W. Reichardt, "Structure of a mechanism of perception of optical movement," *Proceedings of the 1st International Conference on Cybernetics* , pp. 797–801, 1956.
6. H. B. Barlow and W. R. Lewick, "The mechanism of directionally selective units in the rabbit's retina," *Journal of Physiology,* London **178**, pp. 477–504, 1965.
7. F. Ratliff and H. K. Hartline, *Studies on excitation and inhibition in retina*, Chapman and Hall, London, 1974.
8. R. B. Pinter, "Adaptation of receptive field spatial organization via multiplicative lateral inhibition," *Proceedings of the the IEEE Conference on Systems, Man and Cybernetics* , pp. 328–331, 1984.
9. A. Bouzerdoum and R. B. Pinter, "Image motion processing in biological and computer vision systems," *Proceedings of the SPIE Conference on Visual Communications and Image Processing* **1199**, pp. 1229–1240, 1989.
10. G. A. Horridge, "A template theory to relate visual processing," *Proceedings of the Royal Society of London B* **239**, pp. 17–33, 1990.
11. P. Sobey, "Determining range information from self motion - the template model," *Proceedings of the SPIE on Intelligent Robots and Computer Vision* **1382**, pp. 123–131, 1990.

12. A. Moini, A. Bouzerdoum, A. Yakovleff, and K. Eshraghian, "A two dimensional motion detector based on insect vision," *Advanced Focal Plane Arrays and Electronic Cameras,* Berlin, Germany , pp. 146–157, October 1996.
13. A. Moini and A. Bouzerdoum, "A biologically motivated imager and motion detector with pixel level image processing," *Australian Microelectronics Conference,* Melbourne, Australia , pp. 180–185, 29 September-3 November 1997.
14. A. Moini, A. Bouzerdoum, K. Eshraghian, A. Yakovleff, X. T. Nguyen, A. Blanksby, R. Beare, D. Abbott, and R. E. Bogner, "An insect vision based motion detection chip," *IEEE Journal of Solid State Circuits* **32**, pp. 279–284, February 1997.
15. E. H. Adelson and J. Bergen, "Spatiotemporal energy models for the perception of motion," *Journal of the Optical Society of America A* **2**, pp. 284–299, 1985.
16. J. P. van Santen and G. Sperling, "Elaborated Reichardt detectors," *Journal of the Optical Society of America A* **2**, pp. 300–321, 1985.
17. F. Wolf-Oberhollenzer and K. Kirschfeld, "Motion sensitivity in the nucleus of the basal optic root of the pigeon," *Journal of Neurophysiology* **71**, pp. 1559–1573, 1994.
18. R. C. Emerson, M. C. Citron, W. J. Vaughn, and S. A. Klein, "Nonlinear directionally selective subunits in complex cells of cat striate cortex," *Journal of Neurophysiology* **58**, pp. 33–65, 1987.
19. M. Egelhaaf, A. Borst, and W. Reichardt, "Computational structure of a biological motion detection system as revealed by local detector analysis in the fly's nervous system," *Journal of the Optical Society of America A* **6**, pp. 1070–1087, 1989.
20. E. Buchner, "Elementary movement detectors in an insect visual system," *Biological Cybernetics* **24**, pp. 85–101, 1976.
21. M. V. Srinivasan, S. W. Zhang, M. Lehrer, and T. S. Collet, "Honeybee navigation en route to the goal: visual flight control and odometry," *Journal of Experimental Biology* **199**, pp. 237–244, 1996.
22. S. P. McKee, G. H. Silverman, and K. Nakayama, "Precise velocity discrimination despite random variation in temporal frequency and contrast," *Vision Research* **26**, pp. 609–619, 1986.
23. R. O. Dror, "Accuracy of visual velocity estimation by Reichardt correlators," Master's thesis, University of Cambridge, Cambridge, UK, 1998.
24. A. Yakovleff and A. Moini, "Motion perception using analog VLSI," *Journal of Analog Integrated Circuits and Signal Processing* **2**, pp. 1–22, 1997.
25. X. T. Nguyen, A. Bouzerdoum, R. E. Bogner, A. Moini, K. Eshraghian, and D. Abbott, "The stair-step tracking algorithm for velocity estimation," *Proceedings of the Australian New Zealand Conference on Intelligent Information Systems,* Perth, Australia , pp. 412–416, December 1993.
26. A. Yakovleff, X. T. Nguyen, A. Bouzerdoum, A. Moini, R. E. Bogner, and K. Eshraghian, "Dual-purpose interpretation of sensory information," *Proceedings IEEE International Conference on Robotics and Automation,* San Diego, USA, **2**, pp. 1635–1640, May 1994.
27. K. Hausen and M. Egelhaaf, "Neural mechanisms of visual course control in insects," *Facets of vision* , pp. 391–424, 1989.